AIAA SciTech
4-8 January 2016, San Diego, California, USA
AIAA Guidance, Navigation, and Control Conference

An Improved Model-Based Observer for Inertial Navigation for Quadrotors with Low Cost IMUs

David Hanley* and Timothy Bretl †
University of Illinois at Urbana-Champaign, Urbana, IL 61801, USA

In this paper, we present a model-based observer for inertial navigation of quadrotors and other multirotor aircraft. We include in our model a Coriolis term that has been neglected in prior work. Doing so allows us to estimate the entire velocity vector in the quadrotor's frame of reference—including along the z-axis of this frame—with data only from a low-cost inertial measurement unit (IMU): something that has not been demonstrated previously. An observability analysis predicts that our proposed observer will perform well. Experimental results over 110 flight trials verify this prediction, showing that our proposed observer achieves lower root mean square error than three other state-of-the-art model-based observers.

I. Introduction

For several decades now, the well established navigation architecture for aerospace vehicles has been to integrate an inertial measurement unit (IMU) with an externally provided or on-board navigation aid. Typical aided navigation architectures for aerospace vehicles have integrated outputs from the inertial measurement units to produce an accurate a priori measurement that is then used in an observer that corrects errors in the inertial navigation system with the help of the aiding sensor.[1] With respect to the inertial navigation system's algorithms, much of the work over the past few decades has focused on reducing error produced through integration methods.[2–5] In particular, research on integration algorithms have focused primarily on compensating for coning and sculling motion.[6–9]

For small aerial platforms, so-called low cost IMUs have been a popular choice to use in integrated navigation systems due to their small size and weight.[10] These IMUs have been used in conjunction with ultrasonic sensors and magnetometers,[11] lasers,[12,13] GPS,[14,15] and monocular vision.[16] These low cost IMUs, which are typically also microelectromechanical (MEMs) sensors, are usually characterized by a worse turn-on and in-run bias stability than tactical grade and other higher grade IMUs. The turn-on and in-run scale-factor stability of low cost IMUs is typically also worse than these higher grade sensors. Finally, but not exhaustively, these IMUs have a greater sensitivity to temperature changes.

Recently, several researchers have proposed using the dynamics of multirotor helicopters to replace the integrated outputs of a portion of the inertial navigation system with an observer.[17–21] In typical integrated INS methods, errors propagate due to alignment errors (i.e. modeling the IMU in an incorrect frame of reference), sensor errors (i.e. various forms of bias and scale factor errors inherent to the sensors), and computational errors in the integration algorithm.[1] While these observers would actually produce worse state estimates, due to model uncertainty, than the integration methods for navigation grade or even tactical grade IMUs (given a correct initialization), the relatively large sensor errors in low cost IMUs allow these observers to outperform integrated methods. In earlier work, models of a quadrotor in perfect hover were used to estimate attitude. In particular, the accelerometers measure the specific force produced by the thrust of the rotors and this was used to obtain improved pitch and roll measurements.[17] Researchers then proposed that accelerometers in the plane of the propellers actually measure force due to the so called H-force drag. A simplified model of this force is proportional to the velocity of the vehicle in the plane of the rotors.[22] This work was originally used for control of quadrotors, but has since been used for state estimation of vehicle

*Graduate Student, Department of Aerospace Engineering, hanley6@illinois.edu, AIAA Student Member.
†Associate Professor, Department of Aerospace Engineering, tbretl@illinois.edu, AIAA Senior Member.

pitch, roll, and velocities in the plane of a quadrotor's propellers. It has been shown how this H-force drag model improves the quality of the IMU state estimation over both integration methods and the earlier perfect hover assumption.[18–20] Methods have also been proposed to estimate both gyroscope bias and the H-force drag term on-line with only IMU data.[18,19,21] This work has also shown that using this H-force drag model performs better than previously developed models as the correcting rate from an aiding sensor degrades.[20] Researchers have studied how wind and errors in model parameters impact the attitude estimate of an IMU and magnetometer navigation system that also uses the H-force drag in its dynamic model.[23]

In this paper, we present a new observer using only measurements from a low cost IMU on-board a quadrotor. We use the H-force drag model developed in previous work, however, we also include the Coriolis effect in our model. Previous work has either completely omitted any mention of this effect[18] or has ignored it due an assumption that the term is "small enough to be neglected."[19] One justification for assuming the Coriolis effect can be safely ignored is that "the vehicle cannot translate or rotate quickly without rendering exteroceptive sensor data useless."[20] We aim to show in this paper that the Coriolis term can be used to produce substantial improvements over current state-of-the-art observers. This term should not be ignored, because it allows the entire velocity vector in the helicopter frame to be observable, even when the vehicle is not translating or rotating quickly. Current state-of-the-art estimators cannot estimate the entire velocity vector in the helicopter frame. By using the Coriolis term, our observer can do this and produce root mean square errors in the state estimates that are lower than state-of-the-art observers.

In Section II, we present three variants of our observer and three state-of-the-art observers. The difference between these observers is in their model of multirotor helicopters and inertial measurement units. In Section III, we present the nonlinear observability matrix of our proposed observer to show how the entire velocity vector is observable due to the fact that we include the Coriolis effect. We also numerically show how strong the observability properties of our proposed observer are and compare these properties to three state-of-the-art observers. In Section IV, we show results demonstrating the effectiveness of our proposed estimator over 110, thirty second flight trials. Section V offers conclusions and presents future work.

II. System Model and Observer Design

In the previous section, we introduced model-based observers as an alternative to integration of IMU data. We claim that these model-based observers can improve the performance of inertial navigation systems for low cost inertial sensors when compared to integration algorithms. In this section we use a simplified model of the quadrotor and IMU to develop a model-based observer. Then, we introduce three alternative model-based observers presented in existing literature to compare our proposed observer against. Finally, we present two variants of our proposed observer to facilitate this comparison.

A. Proposed Observer

Consider the quadrotor system depicted in Figure 1. We define a world coordinate system $\left(\mathcal{F}^W\right)$ which we shall treat as an inertial frame of reference with an x-axis pointing North, y-axis pointing East, and z-axis pointing in line with the gravity vector. We define the body frame $\left(\mathcal{F}^B\right)$ attached to the quadrotor as shown. We assume that the x-y plane of the body frame is in the plane of the rotors, the origin of this frame is at the center of mass and is also where the IMU is located. We make these assumptions out of convenience. It is relatively straight forward to apply this work when these assumptions are not valid.

In this paper, we use the ZYX Euler angle sequence to express the orientation of the quadrotor. The dynamics of the roll (ϕ), pitch (θ), and yaw (ψ) Euler angles are expressed as

$$\begin{aligned}\dot{\phi} &= \omega_x + \omega_z \tan\theta\cos\phi + \omega_y \tan\theta\sin\phi \\ \dot{\theta} &= \omega_y \cos\phi - \omega_z \sin\phi \\ \dot{\psi} &= \omega_y \frac{\sin\phi}{\cos\theta} + \omega_z \frac{\cos\phi}{\cos\theta}\end{aligned} \tag{1}$$

where ω_x, ω_y, ω_z represent the angular velocities about the x, y, and z-axis respectively.

The acceleration of a general rigid body with respect to an inertial frame written in terms of the body frame coordinate system is

$$\dot{v}^b_{w,b} = \ddot{q}^b_{w,b} + 2\widehat{\omega}^b_{w,b} v^b_{w,b} - \widehat{\omega}^b_{w,b}\widehat{\omega}^b_{w,b} q^b_{w,b} + \dot{\widehat{\omega}}^b_{w,b} q^b_{w,b} \tag{2}$$

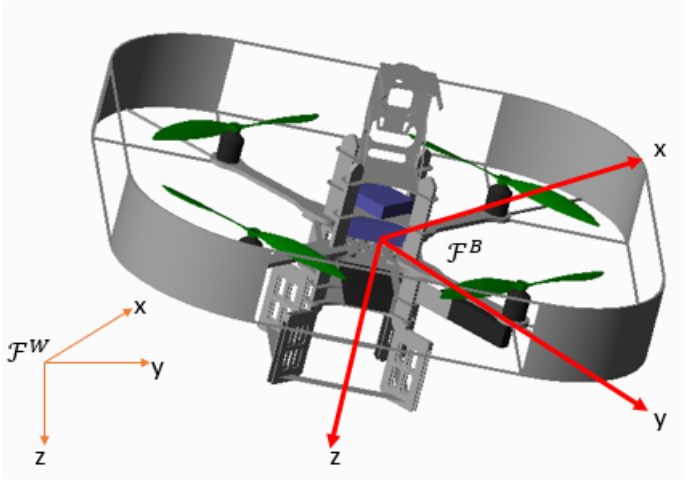

Figure 1. Ascending Technologies Pelican quadrotor with world and body frame.[24]

where $\dot{v}^b_{w,b}$ is the acceleration of the body frame with respect to the world frame written in terms of the body frame, $q^b_{w,b}$ is the position vector, $v^b_{w,b}$ is the velocity vector, $\widehat{\omega}^b_{w,b}$ represents a skew symmetric matrix of the angular velocity vector, $\ddot{q}^b_{w,b}$ is the second time derivative of the position vector, and $\dot{\widehat{\omega}}^b_{w,b}$ is the skew symmetric matrix of the angular acceleration vector.

In this work, we neglect the last two terms of Equation 2, which depend on the position of the body frame with respect to the world frame written in terms of the body frame. We do this because the position of the quadrotor is not, using only an IMU, observable. This results in

$$\dot{v}^b_{w,b} = \frac{F^b}{m} + 2\widehat{\omega}^b_{w,b} v^b_{w,b} \tag{3}$$

where F^b are the forces acting on the quadrotor written in terms of the body frame and m is the mass of the quadrotor.

We assume that gravity, thrust, and the H-force drag term developed in previous literature are the only forces acting on the quadrotor.[18–20,22] For a single propeller rotating with angular velocity ω^p the H-force drag has been modeled as

$$F_H = \omega^p \lambda V_p^{\perp} \tag{4}$$

where F_H is the H-force drag exerted on the rotor, λ is a constant, and $V_p^{\perp}$ is the velocity along the plane of the rotor.[22] Previous work in IMU estimation has simplified this model by assuming the angular velocity of the rotor is approximately constant.[18–20] This results in

$$F_H = \mu V_p^{\perp} \tag{5}$$

which is the model we use in this paper. The resulting dynamic equations of motion are

$$\begin{aligned}
\dot{v}^b_x &= -g\sin\theta - \frac{\mu}{m} v^b_x - 2\omega_z v^b_y + 2\omega_y v^b_z \\
\dot{v}^b_y &= g\cos\theta\sin\phi - \frac{\mu}{m} v^b_y - 2\omega_x v^b_z + 2\omega_z v^b_x \\
\dot{v}^b_z &= g\cos\phi\cos\theta - \frac{T}{m} - 2\omega_y v^b_x + 2\omega_x v^b_y
\end{aligned} \tag{6}$$

where g is standard acceleration due to gravity, μ is the H-force drag constant, T is the thrust produced by the quadrotor's four rotors, v^b_i is the velocity along the i^{th} axis in the body frame, and $\dot{v}^b_i$ is the acceleration along the i^{th} axis in the body frame.

We use a simplified model of the IMU in this work. This model ignores g-dependent bias, anisoelastic, and anisoinertial errors to name a few.[1] This model is

$$\begin{aligned}
a^{SF}_{m_i} &= \lambda_{a_i} a^{SF}_i + \beta_{a_i} + w_{a_i} \\
\omega_{m_i} &= \lambda_{\omega_i} \omega_i + \beta_{\omega_i} + w_{\omega_i}
\end{aligned} \tag{7}$$

where $a^{SF}_{m_i}$ is the specific force measured by the accelerometer along the i^{th} body frame axis, ω_{m_i} is the measured angular velocity about the i^{th} body frame axis, λ_a and λ_ω is the scale factor corrupting the true specific force, a^{SF}, and angular velocity respectively, β_a and β_ω are (potentially time-varying) biases, and w_a and w_ω is a zero mean white Gaussian noise term effecting the accelerometers and gyroscopes.

In our observer, we estimate roll, pitch, and the three body frame velocities. Again, to the best of our knowledge, the observer we propose is the only such observer for multirotor helicopters that can estimate the entire body frame velocity vector with only IMU measurements. We use a standard discrete time extended Kalman filter (EKF) for state estimation; however, other observers can be used as well. The a priori model we use in the EKF is

$$\begin{aligned}
\dot{\breve{\phi}} &= \omega_{m_x} + \omega_{m_z}\tan\breve{\theta}\cos\breve{\phi} + \omega_{m_y}\tan\breve{\theta}\sin\breve{\phi} \\
\dot{\breve{\theta}} &= \omega_{m_y}\cos\breve{\phi} - \omega_{m_z}\sin\breve{\phi} \\
\dot{\breve{v}}^b_x &= -g\sin\breve{\theta} - \frac{\mu}{m}\breve{v}^b_x - 2\omega_{m_z}\breve{v}^b_y + 2\omega_{m_y}\breve{v}^b_z \\
\dot{\breve{v}}^b_y &= g\cos\breve{\theta}\sin\breve{\phi} - \frac{\mu}{m}\breve{v}^b_y - 2\omega_{m_x}\breve{v}^b_z + 2\omega_{m_z}\breve{v}^b_x \\
\dot{\breve{v}}^b_z &= g\cos\breve{\phi}\cos\breve{\theta} + a^{SF}_{m_z}.
\end{aligned} \tag{8}$$

This model uses gyroscope measurements for angular velocity, the z-axis accelerometer measurement, and current state estimates (denoted with a breve). For use in the EKF, Equation 8 must be discretized.

We use the accelerometer output along the body frame x and y-axes as the measurement in the innovation term of the EKF. This innovation term is

$$v = \begin{bmatrix} a^{SF}_{m_x} \\ a^{SF}_{m_y} \end{bmatrix} - \begin{bmatrix} -\frac{\mu}{m}\breve{v}^b_x - 2\omega_{m_z}\breve{v}^b_y + 2\omega_{m_y}\breve{v}^b_z \\ -\frac{\mu}{m}\breve{v}^b_y - 2\omega_{m_x}\breve{v}^b_z + 2\omega_{m_z}\breve{v}^b_x \end{bmatrix}. \tag{9}$$

As a part of the EKF algorithm, we must also take the Jacobian of the a priori model and output model about current state estimates and choose a priori and output model covariances.

B. Previously Developed Observers

We choose to compare our observer to three other observers. Beard, Leishman, and Macdonald presented two observers. They, along with Abeywardena, Kodagoda, Dissanyake, and Munasinghe, showed how using the H-force drag in a quadrotor model provides an improvement over other observers for multirotor helicopters and integration methods for low cost IMUs. To the best of our knowledge, these three observers represent the state-of-the-art INS for multirotor helicopters with low cost IMUs. The first estimator presented by Beard, Leishman, and Macdonald (which we shall call the BLM estimator) uses the a priori model

$$\begin{aligned}
\dot{\breve{\phi}} &= \omega_{m_x} + \omega_{m_z}\tan\breve{\theta}\cos\breve{\phi} + \omega_{m_y}\tan\breve{\theta}\sin\breve{\phi} \\
\dot{\breve{\theta}} &= \omega_{m_y}\cos\breve{\phi} - \omega_{m_z}\sin\breve{\phi} \\
\dot{\breve{v}}^b_x &= -g\sin\breve{\theta} - \frac{\mu}{m}\breve{v}^b_x \\
\dot{\breve{v}}^b_y &= g\cos\breve{\theta}\sin\breve{\phi} - \frac{\mu}{m}\breve{v}^b_y
\end{aligned} \tag{10}$$

and the innovation term[19,20]

$$v = \begin{bmatrix} a^{SF}_{m_x} \\ a^{SF}_{m_y} \end{bmatrix} - \begin{bmatrix} -\frac{\mu}{m}\breve{v}^b_x \\ -\frac{\mu}{m}\breve{v}^b_y \end{bmatrix}. \tag{11}$$

Beard, Leishman, and Macdonald, as an alternative to the BLM estimator, also present an observer that can estimate the H-force drag coefficient as a state parameter in the observer. These researchers show that this drag coefficient is observable as long as the helicopter is experiencing an acceleration in the plane of the rotors. They claim that this observer (which we shall call the BLM-μ observer) allows the user to avoid using complicated parameter identification techniques and expensive motion capture systems.[19] The BLM-μ

observer uses the a priori model

$$\begin{aligned}
\dot{\breve{\phi}} &= \omega_{m_x} + \omega_{m_z}\tan\breve{\theta}\cos\breve{\phi} + \omega_{m_y}\tan\breve{\theta}\sin\breve{\phi} \\
\dot{\breve{\theta}} &= \omega_{m_y}\cos\breve{\phi} - \omega_{m_z}\sin\breve{\phi} \\
\dot{\breve{v}}_x^b &= -g\sin\breve{\theta} - \frac{\breve{\mu}}{m}\breve{v}_x^b \\
\dot{\breve{v}}_y^b &= g\cos\breve{\theta}\sin\breve{\phi} - \frac{\breve{\mu}}{m}\breve{v}_y^b \\
\dot{\breve{\mu}} &= 0
\end{aligned} \tag{12}$$

and the innovation term[19]

$$v = \begin{bmatrix} a_{m_x}^{SF} \\ a_{m_y}^{SF} \end{bmatrix} - \begin{bmatrix} -\frac{\breve{\mu}}{m}\breve{v}_x^b \\ -\frac{\breve{\mu}}{m}\breve{v}_y^b \end{bmatrix}. \tag{13}$$

Both the BLM and BLM-μ observers assume that the gyroscopes measure the angular velocities exactly. Abeywardena, Kodagoda, Dissanyake, and Munasinghe attempt to estimate gyroscope bias about the x and y-axes, in addition to the states estimated by the BLM observer, to improve the performance of their estimator. The a priori model of this observer (which we shall call the AKDM observer) is

$$\begin{aligned}
\dot{\breve{\phi}} &= \omega_{m_x} - \breve{\beta}_{\omega_x} + \omega_{m_z}\tan\breve{\theta}\cos\breve{\phi} + \left(\omega_{m_y} - \breve{\beta}_{\omega_y}\right)\tan\breve{\theta}\sin\breve{\phi} \\
\dot{\breve{\theta}} &= \left(\omega_{m_y} - \breve{\beta}_{\omega_y}\right)\cos\breve{\phi} - \omega_{m_z}\sin\breve{\phi} \\
\dot{\breve{v}}_x^b &= -g\sin\breve{\theta} - \frac{\mu}{m}\breve{v}_x^b \\
\dot{\breve{v}}_y^b &= g\cos\breve{\theta}\sin\breve{\phi} - \frac{\mu}{m}\breve{v}_y^b \\
\dot{\breve{\beta}}_{\omega_x} &= -\frac{\breve{\beta}_{\omega_x}}{\tau_{\omega_x}} \\
\dot{\breve{\beta}}_{\omega_y} &= -\frac{\breve{\beta}_{\omega_y}}{\tau_{\omega_y}}
\end{aligned} \tag{14}$$

and the innovation term is

$$v = \begin{bmatrix} a_{m_x}^{SF} \\ a_{m_y}^{SF} \end{bmatrix} - \begin{bmatrix} -\frac{\mu}{m}\breve{v}_x^b \\ -\frac{\mu}{m}\breve{v}_y^b \end{bmatrix} \tag{15}$$

where τ_{ω_x} and τ_{ω_y} are the time constants of the gyroscope biases.[18] We shall use these three observers, the BLM, BLM-μ, and AKDM, as references against which to compare our proposed observer.

C. Variants of Proposed Observer

In order facilitate comparison between our proposed observer and the BLM, BLM-μ, and AKDM observers, we present two variants of our proposed observer: the proposed-μ variant and the proposed-β variant. Our proposed-μ observer attempts to estimate the H-force drag term as an additional state parameter. The a priori model of this estimator is

$$\begin{aligned}
\dot{\breve{\phi}} &= \omega_{m_x} + \omega_{m_z}\tan\breve{\theta}\cos\breve{\phi} + \omega_{m_y}\tan\breve{\theta}\sin\breve{\phi} \\
\dot{\breve{\theta}} &= \omega_{m_y}\cos\breve{\phi} - \omega_{m_z}\sin\breve{\phi} \\
\dot{\breve{v}}_x^b &= -g\sin\breve{\theta} - \frac{\breve{\mu}}{m}\breve{v}_x^b - 2\omega_{m_z}\breve{v}_y^b + 2\omega_{m_y}\breve{v}_z^b \\
\dot{\breve{v}}_y^b &= g\cos\breve{\theta}\sin\breve{\phi} - \frac{\breve{\mu}}{m}\breve{v}_y^b - 2\omega_{m_x}\breve{v}_z^b + 2\omega_{m_z}\breve{v}_x^b \\
\dot{\breve{v}}_z^b &= g\cos\breve{\phi}\cos\breve{\theta} + a_{m_z}^{SF} \\
\dot{\breve{\mu}} &= 0
\end{aligned} \tag{16}$$

and the innovation term is

$$v = \begin{bmatrix} a^{SF}_{m_x} \\ a^{SF}_{m_y} \end{bmatrix} - \begin{bmatrix} -\frac{\breve{\mu}}{m}\breve{v}^b_x - 2\omega_{m_z}\breve{v}^b_y + 2\omega_{m_y}\breve{v}^b_z \\ -\frac{\breve{\mu}}{m}\breve{v}^b_y - 2\omega_{m_x}\breve{v}^b_z + 2\omega_{m_z}\breve{v}^b_x \end{bmatrix}. \tag{17}$$

Our proposed-β observer attempts to estimate the gyroscope bias terms as an additional state parameter. The a priori model of this estimator is

$$\begin{aligned}
\dot{\breve{\phi}} &= \omega_{m_x} - \breve{\beta}_{\omega_x} + \omega_{m_z}\tan\breve{\theta}\cos\breve{\phi} + \left(\omega_{m_y} - \breve{\beta}_{\omega_y}\right)\tan\breve{\theta}\sin\breve{\phi} \\
\dot{\breve{\theta}} &= \left(\omega_{m_y} - \breve{\beta}_{\omega_y}\right)\cos\breve{\phi} - \omega_{m_z}\sin\breve{\phi} \\
\dot{\breve{v}}^b_x &= -g\sin\breve{\theta} - \frac{\mu}{m}\breve{v}^b_x - 2\omega_{m_z}\breve{v}^b_y + 2\left(\omega_{m_y} - \breve{\beta}_{\omega_y}\right)\breve{v}^b_z \\
\dot{\breve{v}}^b_y &= g\cos\breve{\theta}\sin\breve{\phi} - \frac{\mu}{m}\breve{v}^b_y - 2\left(\omega_{m_x} - \breve{\beta}_{\omega_x}\right)\breve{v}^b_z + 2\omega_{m_z}\breve{v}^b_x \\
\dot{\breve{v}}^b_z &= g\cos\breve{\phi}\cos\breve{\theta} + a^{SF}_{m_z} \\
\dot{\breve{\beta}}_{\omega_x} &= 0 \\
\dot{\breve{\beta}}_{\omega_y} &= 0
\end{aligned} \tag{18}$$

and the innovation term is

$$v = \begin{bmatrix} a^{SF}_{m_x} \\ a^{SF}_{m_y} \end{bmatrix} - \begin{bmatrix} -\frac{\mu}{m}\breve{v}^b_x - 2\omega_{m_z}\breve{v}^b_y + 2\left(\omega_{m_y} - \breve{\beta}_{\omega_y}\right)\breve{v}^b_z \\ -\frac{\mu}{m}\breve{v}^b_y - 2\left(\omega_{m_x} - \breve{\beta}_{\omega_x}\right)\breve{v}^b_z + 2\omega_{m_z}\breve{v}^b_x \end{bmatrix}. \tag{19}$$

In the proposed-β model, we assume the bias term is constant. Abeywardena, Kodagoda, Dissanayake, and Munasinghe do not provide a means by which they estimate their time constants, so we simply omit them in our proposed-β observer and take the limit as the time constant goes to infinity in the AKDM observer. Note again that our proposed observer, and its variants, estimate the entire velocity vector in the body frame of reference. The BLM, BLM-μ, and AKDM observers estimate only two of the three elements of this velocity vector. As we will show, this difference will cause our proposed estimator to substantially outperform our benchmark estimators. In the next section, we shall study the observability properties of the BLM, BLM-μ, AKDM, and the proposed observer and its variants. In Section IV we shall present metrics by which we will compare these estimators and we shall show how our proposed estimator outperforms its benchmark observers.

III. Observability Analysis

In the previous section, we developed a model-based observer that includes the Coriolis term in its model. We then presented three alternative models described in previous work and two additional variants of the observer we developed to facilitate comparison with the alternative observers. In this section we begin the comparison with a study of the observability properties of these six models. It is obvious that using even the simplified accelerometer and gyroscope model presented in Equation 7 implies that all the models presented would, in fact, be technically unobservable. This is due to the fact that there exists an unknown scale factor and time varying unknown bias term for every measurement. Previous work uses simplified models of the IMU to show observability with the assumption that observers are robust to these small disturbances. We begin by exploring the use of the observability rank condition with our observer as done in previous work. We find this method rather lacking, however, because it does not indicate how easy it is to observe a system. We use two metrics presented by Krener and Ide to measure the strength of the observability of the proposed estimators.[25] From these metrics we believe the performance of the estimators can be inferred even in the presence of small disturbances. Alternatively, we could have used a sensitivity analysis similar to that presented by Hernandez, Tsotsos, and Soatto for vision-aided inertial navigation systems to find a bound on the set of indistinguishable state trajectories.[26]

A. Observability Rank Condition

Previous work on observability analysis for this type of system used the observability rank condition to establish which states are locally, weakly observable when the quadrotor is near its hover condition.[19,20] This type of rank condition states that a nonlinear system described by

$$\begin{aligned} \dot{x} &= f(x,u), \quad x \in \mathbb{R}^n,\, u \in \mathbb{R}^m \\ y &= g(x), \quad y \in \mathbb{R}^p \end{aligned} \tag{20}$$

and observability matrix defined by

$$\begin{gathered} \mathcal{O} = \begin{bmatrix} dg(x) \\ \vdots \\ dL_f^k(g)(x) \end{bmatrix} \\ \text{where} \quad dL_f^k(g)(x) = dL_f^{k-1}(g)(x) f(x,u), \quad dL_f^0(g)(x) = dg(x), \\ \text{and} \quad dg(x) = \frac{\partial g}{\partial x}(x) \end{gathered} \tag{21}$$

is locally, weakly observable if the rank of the observability matrix is equal to the number of states (n).[27] Note that for real analytic systems, this observability rank condition is a necessary and sufficient condition for observability.

We have computed the first four rows of the observability matrix for the BLM observer as

$$\mathcal{O}_{BLM} = \begin{bmatrix} 0 & 0 & -\frac{\mu}{m} & 0 \\ 0 & 0 & 0 & -\frac{\mu}{m} \\ 0 & \frac{g\mu\cos\theta}{m} & \frac{\mu^2}{m^2} & 0 \\ -\frac{g\mu\cos\phi\cos\theta}{m} & \frac{g\mu\sin\phi\sin\theta}{m} & 0 & \frac{\mu^2}{m^2} \end{bmatrix}. \tag{22}$$

From this subset of the observability matrix, it is can be inferred that the BLM system is observable everywhere except where $\phi = \frac{\pi}{2}$ or $\theta = \frac{\pi}{2}$ since the first column of the fourth row element will be zero. However, we cannot prove that without the full observability matrix. Next we computed the first five rows of the observability matrix for the BLM-μ observer. This matrix is

$$\mathcal{O}_{BLM-\mu} = \begin{bmatrix} 0 & 0 & -\frac{\mu}{m} & 0 & -\frac{v_x}{m} \\ 0 & 0 & 0 & -\frac{\mu}{m} & -\frac{v_y}{m} \\ 0 & \frac{g\mu\cos\theta}{m} & \frac{\mu^2}{m^2} & 0 & \frac{2\mu v_x + gm\sin\theta}{m^2} \\ -\frac{g\mu\cos\phi\cos\theta}{m} & \frac{g\mu\sin\phi\sin\theta}{m} & 0 & \frac{\mu^2}{m^2} & \frac{2\mu v_y - gm\cos\theta\sin\phi}{m^2} \\ \frac{g\mu\cos\theta(-\omega_z\cos\phi - \omega_y\sin\phi)}{m} & \mathcal{O}_{(5,2)} & -\frac{\mu^3}{m^3} & 0 & \mathcal{O}_{(5,5)} \end{bmatrix} \tag{23}$$

where

$$\begin{aligned} \mathcal{O}_{(5,2)} &= -\frac{g\mu^2\cos\theta}{m^2} - \frac{g\mu\left(\omega_y\cos\phi - \omega_z\sin\phi\right)\sin\theta}{m} \\ \mathcal{O}_{(5,5)} &= -\frac{\mu^2 v_x}{m^3} + \frac{g\cos\theta\left(\omega_y\cos\phi - \omega_z\sin\phi\right)}{m} + \frac{2\mu\left(-\frac{\mu v_x}{m} - g\sin\theta\right)}{m^2}. \end{aligned} \tag{24}$$

From this matrix, it appears that there may be several unobservable modes. For example, when ω_x and ω_y are zero and $\phi = \frac{\pi}{2}$ or $\theta = \frac{\pi}{2}$. Another unobservable state is when $\phi = 0$, $\theta = \frac{\pi}{2}$, and $\omega_y = 0$. Again, while we can hypothesize that these may be unobservable states, we would need the full observability matrix to prove this is true. Beard, Leishman, and Macdonald presented a similar analysis where they claimed that the system becomes unobservable when the acceleration along the plane of the rotors become zero.[19] Next we computed the first six rows of the observability matrix for the AKDM observer. This matrix is

$$\mathcal{O}_{AKDM} = \begin{bmatrix} 0 & 0 & -\frac{\mu}{m} & 0 & 0 & 0 \\ 0 & 0 & 0 & -\frac{\mu}{m} & 0 & 0 \\ 0 & \frac{g\mu\cos\theta}{m} & \frac{\mu^2}{m^2} & 0 & 0 & 0 \\ -\frac{g\mu\cos\phi\cos\theta}{m} & \frac{g\mu\sin\phi\sin\theta}{m} & 0 & \frac{\mu^2}{m^2} & 0 & 0 \\ \mathcal{O}_{(5,1)} & \mathcal{O}_{(5,2)} & -\frac{\mu^3}{m^3} & 0 & -\frac{\mu^2}{m^2} & -\frac{g\mu\cos\phi\cos\theta}{m} \\ \mathcal{O}_{(6,1)} & \mathcal{O}_{(6,2)} & 0 & -\frac{\mu^3}{m^3} & \frac{g\mu\cos\phi\cos\theta}{m} & 0 \end{bmatrix} \tag{25}$$

where

$$\mathcal{O}_{(5,1)} = -\frac{g\mu\cos\theta\left(\omega_z\cos\phi + (-\beta_y+\omega_y)\sin\phi\right)}{m}$$
$$\mathcal{O}_{(5,2)} = \frac{g\mu\left(-\mu\cos\theta + m\left((\beta_y-\omega_y)\cos\phi+\omega_z\sin\phi\right)\sin\theta\right)}{m^2}$$
$$\mathcal{O}_{(6,1)} = \frac{g\mu\cos\theta\left(\mu\cos\phi + m\left(-\beta_x+\omega_x\right)\sin\phi\right)}{m^2}$$
$$\mathcal{O}_{(6,2)} = -\frac{g\mu\left(m\omega_z\cos\theta + \left(m\left(\beta_x-\omega_x\right)\cos\phi+\mu\sin\phi\right)\sin\theta\right)}{m^2}.$$

Finally, we computed the first five rows of our proposed observer's observability matrix as

$$\mathcal{O}_{prop} = \begin{bmatrix} 0 & 0 & -\frac{\mu}{m} & -2\omega_z & 2\omega_y \\ 0 & 0 & 2\omega_z & -\frac{\mu}{m} & -2\omega_x \\ \mathcal{O}_{(3,1)} & \mathcal{O}_{(3,2)} & \frac{\mu^2}{m^2}-4\omega_z^2 & \frac{4\mu\omega_z}{m} & -\frac{2\mu\omega_y}{m}+4\omega_x\omega_z \\ \mathcal{O}_{(4,1)} & \mathcal{O}_{(4,2)} & -\frac{4\mu\omega_z}{m} & \frac{\mu^2}{m^2}-4\omega_z^2 & \frac{2\mu\omega_x}{m}+4\omega_y\omega_z \\ \mathcal{O}_{(5,1)} & \mathcal{O}_{(5,2)} & \mathcal{O}_{(5,3)} & \mathcal{O}_{(5,4)} & \mathcal{O}_{(5,5)} \end{bmatrix} \tag{26}$$

where

$$\mathcal{O}_{(3,1)} = -2g\omega_z\cos\phi\cos\theta - 2g\omega_y\cos\theta\sin\phi$$
$$\mathcal{O}_{(3,2)} = \frac{g\mu\cos\theta}{m} - 2g\omega_y\cos\phi\sin\theta + 2g\omega_z\sin\phi\sin\theta$$
$$\mathcal{O}_{(4,1)} = -\frac{g\mu\cos\phi\cos\theta}{m} + 2g\omega_x\cos\theta\sin\phi$$
$$\mathcal{O}_{(4,2)} = -2g\omega_z\cos\theta + 2g\omega_x\cos\phi\sin\theta + \frac{g\mu\sin\phi\sin\theta}{m}$$
$$\mathcal{O}_{(5,1)} = -\frac{g\cos\theta\left((2m\omega_x\omega_y-3\mu\omega_z)\cos\phi+(-\mu\omega_y+2m\omega_x\omega_z)\sin\phi\right)}{m}$$
$$\mathcal{O}_{(5,2)} = \frac{-g\left(\mu^2+2m^2\left(\omega_y^2-\omega_z^2\right)\right)\cos\theta}{m^2} + \ldots$$
$$\frac{gm\left((\mu\omega_y-2m\omega_x\omega_z)\cos\phi+(2m\omega_x\omega_y-3\mu\omega_z)\sin\phi\right)\sin\theta}{m^2}$$
$$\mathcal{O}_{(5,3)} = \frac{8\mu\omega_z^2-\mu\left(\frac{\mu^2}{m^2}-4\omega_z^2\right)}{m}$$
$$\mathcal{O}_{(5,4)} = -\frac{4\mu^2\omega_z}{m^2} - 2\omega_z\left(\frac{\mu^2}{m^2}-4\omega_z^2\right)$$
$$\mathcal{O}_{(5,5)} = -\frac{8\mu\omega_x\omega_z}{m} + 2\omega_y\left(\frac{\mu^2}{m^2}-4\omega_z^2\right).$$

The proposed-μ and proposed-β observability matrices have been omitted here due to their length. We find the analysis of these estimators with observability matrices insufficient for comparison. First, none of the matrices presented display the full observability matrix of a system. The rank condition generally only indicates whether or not the system is observable. The analysis we presented may allow us to infer what some unobservable modes may be, but we cannot guarantee that this is actually the case. In particular, we may identify some observable modes as unobservable. Finally, we have no indication with the observability rank condition how easy it will be for an observer to accurately estimate the states of a system.

In the following chapter, we use two measures of the degree of observability presented in previous literature and use them to compare the six observers. These measurements use the singular values of the observability Gramian about a nominal trajectory. Recall that we claim including the Coriolis term in our proposed model allows the entire velocity vector to become observable in the body frame. Also, we can infer (through substitution), from Equation 26 that the proposed observer experiences an unobservable mode when ω_x, ω_y, and ω_z is zero. We also infer from Equation 26 that the observability of the system is not dependent on the thrust produced by the quadrotor over some time interval. These inferences will be used to establish nominal trajectories.

B. Degree of Observability

We shall use the so-called local unobservability index and local estimation condition number to assess observability. Since the observability rank condition does not imply how hard it is to observe the system, we use these metrics to allow us to make better conclusions about the observability properties of the system. The local unobservability index is defined as the reciprocal of the smallest local singular value of the local observability gramian defined as

$$P(x^0) = \int_0^{t_f} \Phi^T(t) G^T(t) G(t) \Phi(t) dt \tag{27}$$

where

$$G(t) = \frac{\partial g}{\partial x}(x^0(t))$$

t_f is the final time, and Φ is the fundamental matrix of the system linearized about a nominal trajectory. This local unobservability index measures how difficult it is to observe the initial state from the system's outputs. The local estimation condition number is defined as the ratio of the largest local singular value to the smallest local singular value and is a measure of how much a small change in the initial condition of one state effects the change in the output relative to small changes in the initial conditions of other states. In other words, it becomes more challenging to design an effective observer as the local unobservability index and the local estimation condition number grows.[25]

In this paper, we compute the local observability gramian numerically. First, we choose a nominal trajectory and a small scalar $\rho > 0$. Then, we compute perturbed trajectories as described (using the notation presented by Kang, Krener, Xiao, and Xu) in

$$\begin{aligned} \dot{x}^{\pm}(t) &= f(x^{\pm}(t), u(t)) \\ x^{\pm}(0) &= x_0 \pm \rho v_i \end{aligned} \tag{28}$$

where the set of vectors v_1, v_2, $\cdots$, v_n form an orthonormal basis in $\mathbb{R}^n$. Finally, we compute the local observability gramian with[28]

$$P_{ij} = \int_0^{t_f} \Delta_i^T(t) \Delta_j(t) dt \tag{29}$$

where

$$\Delta_i(t) = \frac{1}{2\rho}(g(x^+(t)) - g(x^-(t))).$$

Note that as $\rho \to 0$ the numerical approximation approaches the true local observability Gramian. Note that when one or more of the singular values of this observability Gramian is zero, this system is unobservable.

We now compare the observability properties of the BLM, BLM-μ, and AKDM observers with the proposed observer and its variants. In our rank condition analysis, we found that the observability of our system is not directly dependent on the thrust produced by the system, but our proposed observer and its variants are dependent on the angular velocities. Therefore, we produce nominal trajectories by beginning with an initial state (all states zero except for μ which we choose as 0.8281), setting thrust equal to the weight of the quadrotor, and then varying the angular velocity about each axis according to the function

$$\omega_i = \epsilon \sin(1.25t) \quad \text{where} \quad i = x, y, z. \tag{30}$$

One way to interpret Equation 30 is as a deterministic model of a disturbance the quadrotor may experience in hover. We plot the unobservability index as a function of ϵ for $\rho = 0.0001$ in Figure 2(a). First, note that for all $\epsilon > 0$, all proposed systems are observable. The observability properties of the BLM and AKDM observers appear to be independent of ϵ. Additionally, all observers appear to converge to the same unobservability index near $\epsilon = 0.1$. The proposed estimator appears to have a high unobservability index until approximately $\epsilon = 0.001$ when it begins to drop rapidly relative to the BLM-μ, proposed-β, and proposed-μ observers. The condition number for the proposed-β estimator is consistently higher than the alternative estimators. The AKDM conditition number is consistently at least two orders of magnitude larger than the BLM observer. The AKDM also appears to have a larger condition number than the proposed, BLM-μ, and proposed-μ observers for $\epsilon > 0.01$.

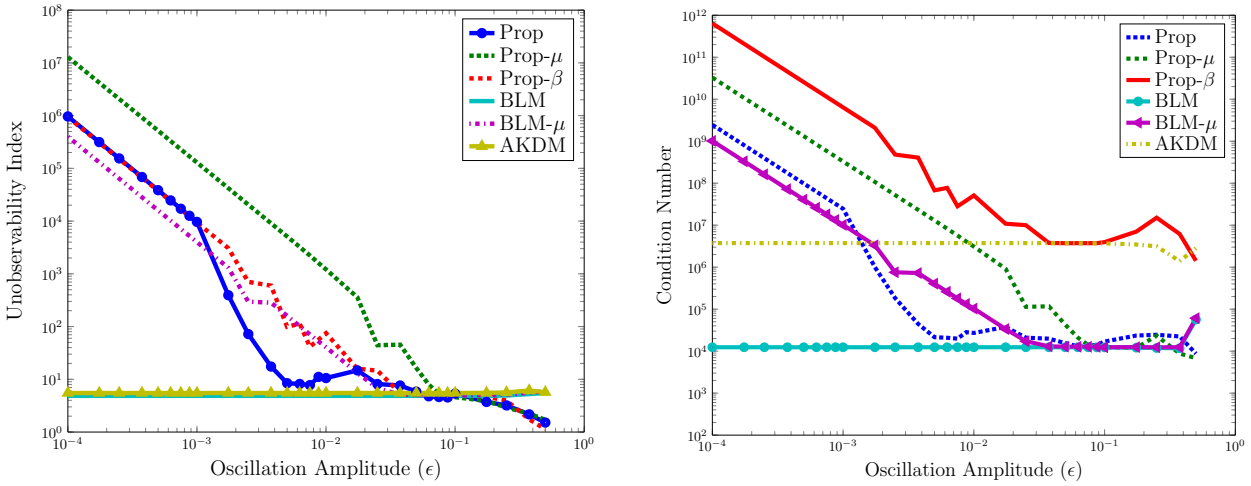

(a) Unobservability Index

(b) Estimation Condition Number

Figure 2. Observability Properties of Presented Observers. Lower unobservability indices and estimation condition numbers imply that it is easier for an observer to accurately estimate the true states of the system.

As mentioned previously, the inherent advantage of our proposed observer and its variants are the potential for the entire velocity vector to be accurately estimated. As shown, this can only happen if the angular velocities are high enough during any flight conditions the quadrotor may experience such that an observer can be used to accurately estimate the states of the quadrotor. In Section IV, we will evaluate these observers over 110, thirty second flight trials and discuss these results in the context of their observability properties.

IV. Flight Tests and Results

In the previous section, we compared the observability properties of the six observers. In this section, we implement these observers in flight tests. These observability properties provide context to these results and some degree of explanatory power. Flight tests were conducted on an Ascending Technologies Pelican quadrotor. Accelerometer and gyroscope data was collected along with position and orientation from a set of 24 Flex 3 Optitrack motion capture cameras with a roughly 100 Hz frame rate over 13 manual flights. Pairs of these cameras (one approximately 2 feet below the other) were distributed around a 40 ft $\times$ 30 ft $\times$ 9 ft room. These thirteen flights are broken into 110, 30 second trials. We estimate the H-force drag off-line for all thirteen flights and average the results over all data points. The H-force drag was estimated to be 0.828. We first present an illustration of our results for one trial and then present the aggregated root mean square error results for all 110 trials.

A. Illustration of Observers

Figure 3(a) shows the absolute value of the error in the estimate of velocity along the body frame z-axis in both the integrated case and for the proposed estimator. Note that for the BLM, BLM-μ, and AKDM observers, the body frame z-axis velocity must be computed by integrating accelerometer measurements and compensating for gravity. The improvement the proposed estimator provides is obvious. While the error in the proposed estimator is not zero, it is better: even for very short time scales. For this particular trial, the RMS error of velocity along the body frame z-axis is 0.115 meters per second for the proposed estimator. Meanwhile, the RMS error of velocity along the body frame x and y-axes are 0.316 and 0.378 meters per second respectively for the proposed estimator.

Figure 3(b) also shows substantial improvements in the position estimate of the quadrotor over a 30 second period caused by the proposed estimator versus the BLM observer. Here the norm of the error in the position estimate with the proposed observer is approximately 100 meters smaller over thirty seconds than with the BLM estimator. The true positions of the quadrotor over this trial are shown in Figure 3(c). This result is due to the substantial improvement in the body frame z-axis velocity estimate, whose error is

almost eight meters per second smaller in the proposed estimator after thirty seconds than with the BLM estimator. While we only show these results for one trial, these results are reflective of what we see over the 110 trials as a whole.

Figure 3(d) shows the position estimates for the BLM-μ and proposed-μ estimators together. For most of the flight, the proposed-μ estimator's position error norm grows at a much slower rate than the BLM-μ. As with the proposed estimator, this is due to the fact that we can leverage the Coriolis effect to estimate the body frame Z velocity. Toward the end of the flight, however, the proposed-μ observer has a very sudden growth in its position error norm. The results from both the BLM-μ and proposed-μ observers are much less consistent across the 110 trials than the BLM and proposed estimators' results. Figure 3(e) shows the norm of the position error for the BLM-μ and proposed-μ observers for a different trial. These results are quite different from 3(d) since the proposed-μ position error is significantly smaller than the BLM-μ error after thirty seconds.

Figure 3(f) compares the norm of the position error of the AKDM observer with the proposed-β estimate. Again the norm of the error in the position estimate with the proposed-β observer is approximately 100 meters smaller over thirty seconds than with the AKDM estimator. Like with the results from Figure 3(b) this result is due to the substantial improvement in the body frame z-axis velocity estimate.

B. Results Over 110 Trials

We aggregate the results for 110, thirty second trials into the following tables: Table 1 shows the average root mean square (RMS) error for each estimator over 110 cases, Table 2 presents the maximum and minimum RMS error over the trials, and Table 3 presents the standard deviation of the trials. First, note that the proposed and proposed-β observers have both a lower average RMS error and standard deviation for the body frame z-axis velocity than the BLM, BLM-μ, and AKDM observers. Also, the maximum RMS error is lower for the proposed and proposed-β observers than the minimum RMS error for the BLM, BLM-μ, and AKDM observers. This is due to the fact that including the Coriolis term in our model has enabled us to effectively estimate this additional state rather than using simple integration that is used in the BLM, BLM-μ, and AKDM observers.

By almost every metric, the proposed-μ estimator is by far the worst of the six estimators presented at observing the velocity vector. Note that this is due to the tendency of this proposed-μ observer to become unstable with respect to error. The median RMS error of the body frame z-axis velocity is only 0.211 meters per second however. Again, this is lower than the minimum error shown for observers that do not leverage the Coriolis effect. It is not surprising that the proposed-μ observer had some unstable results. Figure 2 shows how this observer has consistently the worst local unobservability index of all the observers presented.

There is no clear improvement or harm produced by using the AKDM compared to the BLM or the proposed-β compared to the proposed observers. With regard to several metrics (i.e. the velocity along the y-axis) these bias observing estimators do worse than their alternatives. However, the average RMS error of velocity along the x-axis is smallest for the AKDM observer. While the bias of low cost IMUs are high relative to higher grade sensors, these values are still typically small compared to the other states and angular velocities. This fact, along with the relatively high condition number of the AKDM and proposed-β observers, make it difficult to accurately estimate the gyroscope bias.

Estimator	RMS Roll Error (rad)	RMS Pitch Error (rad)	RMS v_x^b Error (m/s)	RMS v_y^b Error (m/s)	RMS v_z^b Error (m/s)
Proposed	0.120	0.083	0.351	0.384	0.169
BLM	0.143	0.090	0.352	0.542	4.474
Proposed-μ	0.119	0.109	6.125×10^{10}	1.106×10^{13}	1.372×10^{8}
BLM-μ	0.289	0.218	8.682	14.667	15.750
Proposed-β	0.126	0.083	0.348	0.396	0.171
AKDM	0.136	0.088	0.335	0.552	4.814

Table 1. Average RMS Error in Estimators

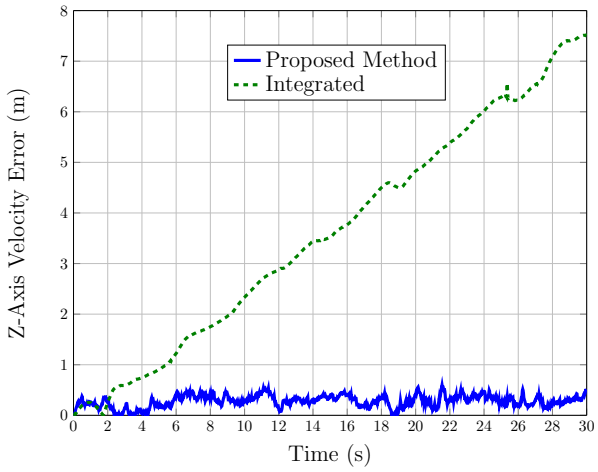

(a) Error Along Body Frame z-Axis

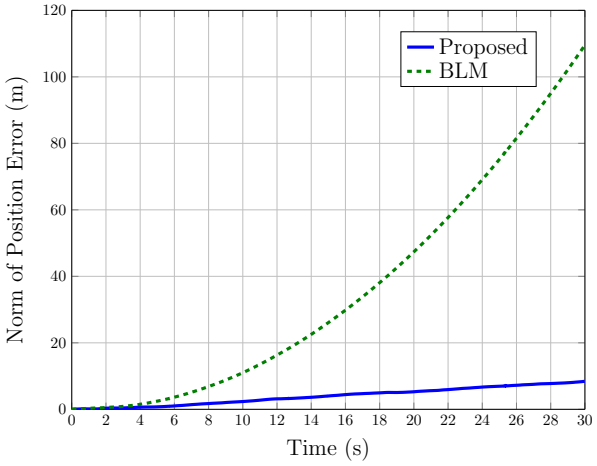

(b) Error in Position of BLM and Proposed Estimator

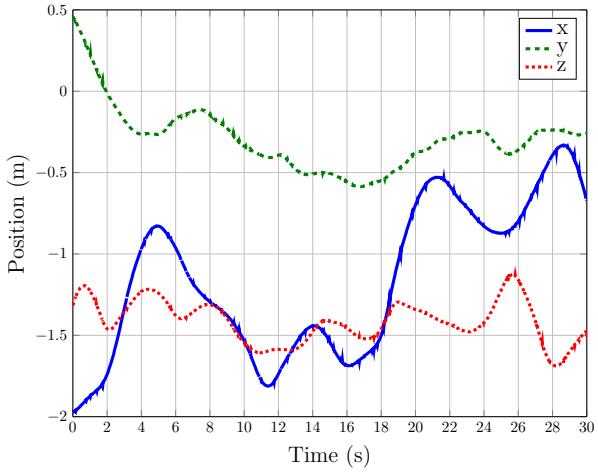

(c) Motion Capture Position

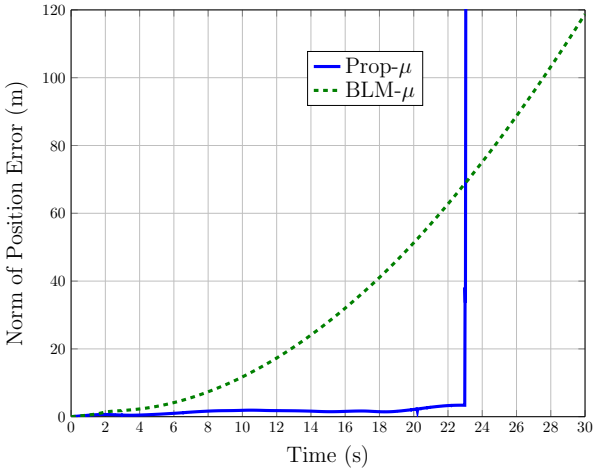

(d) Error in Position of BLM-μ and Proposed-μ Estimator

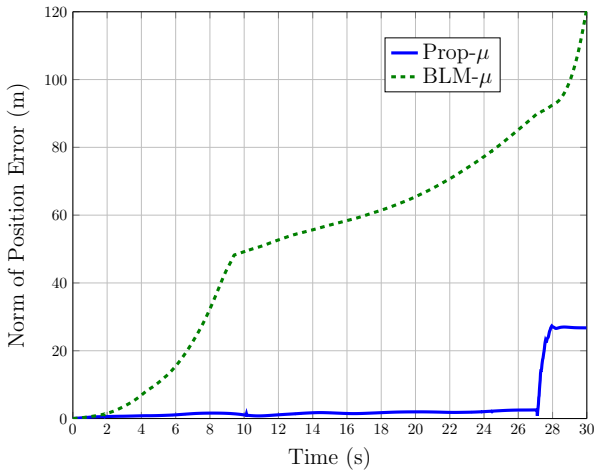

(e) Case of Smaller Error in Position of Proposed-μ Compared with BLM-μ Estimator After 30 Seconds

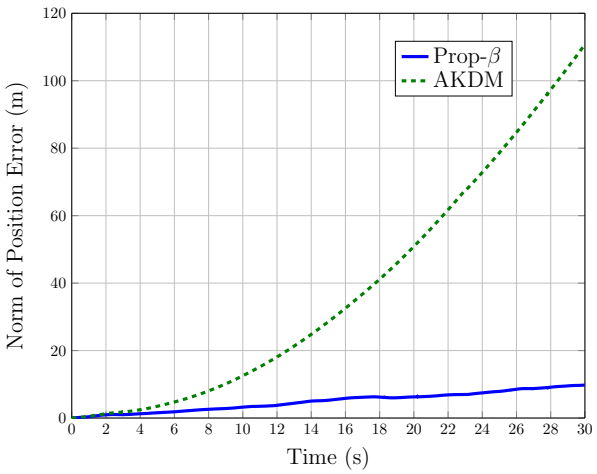

(f) Error in Position of AKDM and Proposed-β Estimator

Figure 3. Illustration of Estimator Results

Estimator	RMS Roll Error (rad)		RMS Pitch Error (rad)		RMS v_x^b Error (m/s)		RMS v_y^b Error (m/s)		RMS v_z^b Error (m/s)	
Proposed	0.509	0.034	0.263	0.027	0.634	0.147	0.628	0.243	0.271	0.095
BLM	0.980	0.035	0.283	0.025	0.641	0.119	0.969	0.337	18.032	0.662
Proposed-μ	0.778	0.024	1.068	0.018	6.109×10^{12}	0.098	1.106×10^{15}	0.057	1.371×10^{10}	0.110
BLM-μ	1.080	0.026	0.825	0.020	113.220	0.095	220.626	0.075	76.788	1.400
Proposed-β	0.519	0.035	0.236	0.026	0.623	0.140	0.572	0.251	0.276	0.095
AKDM	0.517	0.035	0.410	0.027	0.628	0.114	0.841	0.343	18.718	0.471

Table 2. Maximum/Minimum RMS Error in Estimators

Estimator	RMS Roll Error (rad)	RMS Pitch Error (rad)	RMS v_x^b Error (m/s)	RMS v_y^b Error (m/s)	RMS v_z^b Error (m/s)
Proposed	0.074	0.047	0.123	0.072	0.041
BLM	0.119	0.054	0.148	0.109	2.967
Proposed-μ	0.108	0.141	6.109×10^{11}	1.106×10^{14}	1.371×10^{9}
BLM-μ	0.243	0.195	14.365	25.970	17.945
Proposed-β	0.073	0.046	0.124	0.074	0.042
AKDM	0.081	0.058	0.136	0.107	3.404

Table 3. Standard Deviation of RMS Error in Estimators

V. Conclusions

In this paper, we have presented an observer that leverages a model of a quadrotor and IMU data to compute roll, pitch, and the body frame velocity vector. The observer is able to effectively estimate one more state than previously presented observers. We have shown through analysis of the observability properties of the proposed observer and through flight tests that this observer will perform well over reasonable flight conditions. We have also shown, again through observability analysis and through flight tests, that it is ineffective to estimate either the H-force or gyroscope biases as part of our estimator. For low cost IMUs, we believe the proposed observer can substantially improve the performance of the inertial navigation capabilities of multirotor unmanned aircraft. This is immediately applicable in environments where the time between updated navigation data from an aiding sensor becomes longer or when the aiding sensor experiences a fault. In the future we shall explore integrating this method for inertial navigation with aiding sensors such as a monocular camera.

Acknowledgments

This work is supported in part by the National Science Foundation Grant No. 14-46765 and 14-27111.

References

[1]Titterton, D. and Weston, J., *Strapdown Inertial Navigation Technology*, Vol. 17 of *Radar, Sonar, Navigation and Avionics Series*, The Institution and Engineering and Technology, 2nd ed., 2004.

[2]Savage, P. G., "Strapdown Inertial Navigation Integration Algorithm Design Part 1: Attitude Algorithms," *Journal of Guidance, Control, and Dynamics*, Vol. 21, No. 1, January 1998, pp. 19–28.

[3]Savage, P. G., "Strapdown Inertial Navigation Integration Algorithm Design Part 2: Velocity and Position Algorithms," *Journal of Guidance, Control, and Dynamics*, Vol. 21, No. 2, March 1998, pp. 208–221.

[4]Savage, P. G., "A Unified Mathematical Framework for Strapdown Algorithm Design," *Journal of Guidance, Control, and Dynamics*, Vol. 29, No. 2, March 2006, pp. 237–249.

[5]Litmanovich, Y. A., Lesyuchevsky, V. M., and Gusinsky, V. Z., "Two New Classes of Strapdown Navigation Algorithms," *Journal of Guidance, Control, and Dynamics*, Vol. 23, No. 1, January 2000, pp. 34–44.

[6]Ignagni, M. B., "Optimal Strapdown Attitude Integration Algorithms," *Journal of Guidance, Control, and Dynamics*, Vol. 13, No. 2, March 1990, pp. 363–369.

[7]Savage, P. G., "Explicit Frequency-Shaped Coning Algorithms for Pseudoconing Environments," *Journal of Guidance,*

Control, and Dynamics, Vol. 34, No. 3, May 2011, pp. 774–782.

[8]Savage, P. G., "Coning Algorithm Design by Explicit Frequency Shaping," *Journal of Guidance, Control, and Dynamics*, Vol. 33, No. 4, July 2010, pp. 1123–1132.

[9]Savage, P. G., "Strapdown Sculling Algorithm Design for Sensor Dynamic Amplitude and Phase-Shift Error," *Journal of Guidance, Control, and Dynamics*, Vol. 35, No. 6, November 2012, pp. 1718–1729.

[10]Chao, H., Coopmans, C., Di, L., and Chen, Y. Q., "A Comparative Evaluation of Low-Cost IMUs for Unmanned Autonomous Systems," *Proceedings of the IEEE International Conference on Multisensor Fusion and Integration for Intelligent Systems*, Salt Lake City, Utah, September 2010, pp. 211–216.

[11]Zhao, H. and Wang, Z., "Motion Measurement Using Inertial Sensors, Ultrasonic Sensors, and Magnetometers with Extended Kalman Filter for Data Fusion," *IEEE Sensors Journal*, Vol. 12, No. 5, May 2012, pp. 943–953.

[12]Sa, I. and Corke, P., "System Identification, Estimation and Control for a Cost Effective Open-Source Quadcopter," *IEEE International Conference on Robotics and Automation*, RiverCentre, Saint Paul, Minnesota, USA, May 2012, pp. 2202–2209.

[13]Grzonka, S., Grisetti, G., and Burgard, W., "Towards a Navigation System for Autonomous Indoor Flying," *IEEE International Conference on Robotics and Automation*, Kobe International Conference Center, Kobe, Japan, May 2009, pp. 2878–2883.

[14]Kingston, D. B. and Beard, R. W., "Real-Time Attitude and Position Estimation for Small UAVs Using Low-Cost Sensors," *AIAA "Unmanned Unlimited" Technical Conference, Workshop and Exhibit*, Chicago, Illinois, September 2004.

[15]Tailanian, M., Paternain, S., Rosa, R., and Canetti, R., "Design and Implementation of Sensor Data Fusion for an Autonomous Quadrotor," *IEEE Instrumentation and Measurement Technology Conference*, Montevideo, Uruguay, May 2014, pp. 1431–1436.

[16]Scaramuzza, D., Achtelik, M. C., Doitsidis, L., Fraundorfer, F., Kosmatopoulos, E., Martinelli, A., Achtelik, M. W., Chli, M., Chatzichristofis, S., Kneip, L., Gurdan, D., Heng, L., Lee, G. H., Lynen, S., Meier, L., Pollefeys, M., Renzaglia, A., Siegwart, R., Stumpf, J. C., Tanskanen, P., Troiani, C., and Weiss, S., "Vision-Controlled Micro Flying Robots: From System Design to Autonomous Navigation and Mapping in GPS-Denied Environments," *IEEE Robotics and Automation Magazine*, September 2014, pp. 26–40.

[17]Abeywardena, D. M. W. and Munasinghe, S. R., "Performance Analysis of a Kalman Filter Based Attitude Estimator for a Quad Rotor UAV," *IEEE International Congress on Ultra Modern Telecommunications and Control Systems Workshops*, Moscow, Russia, October 2010, pp. 466–471.

[18]Abeywardena, D., Kodagoda, S., Dissanayake, G., and Munasinghe, R., "Improved State Estimation in Quadrotor MAVs," *IEEE Robotics and Automation Magazine*, 2013.

[19]Leishman, R. C., MacDonald, J. C., Beard, R. W., and Mclain, T. W., "Quadrotors and Accelerometers: State Estimation with an Improved Dynamic Model," *IEEE Control Systems Magazine*, 2014.

[20]Macdonald, J., Leishman, R., Beard, R., and Mclain, T., "Analysis of an Improved IMU-Based Observer for Multirotor Helicopters," *Journal of Intelligent and Robotic Systems*, 2014.

[21]Sanz, R., Rodenas, L., Garcia, P., and Castillo, P., "Improving Attitude Estimation Using Inertial Sensors for Quadrotor Control Systems," *International Conference on Unmanned Aircraft Systems*, Orlando, Florida, May 2014, pp. 895–901.

[22]Martin, P. and Salaun, E., "The True Role of Accelerometer Feedback in Quadrotor Control," *IEEE International Conference on Robotics and Automation*.

[23]Baranek, R. and Solc, F., "Model-Based Attitude Estimation for Multicopters," *Advances in Electrical and Electronic Engineering*, 2014.

[24]Guimares, D. L., "Ascending Technologies Pelican CAD Model," http://wiki.asctec.de/display/AR/CAD+Models.

[25]Krener, A. J. and Ide, K., "Measures of Unobservability," *Proceedings of the 48th IEEE Conference on Decision and Control*, Shanghai, December 2009.

[26]Hernandez, J., Tsotos, K., and Soatto, S., "Observability, Identifiability and Sensitivity of Vision-Aided Inertial Navigation," *Proceedings of the International Conference on Robotics and Automation (ICRA)*, May 2015.

[27]Hermann, R. and Krener, A. J., "Nonlinear Controllability and Observability," *IEEE Transactions on Automatic Control*, Vol. 22, 1977, pp. 728–740.

[28]Kang, W., Krener, A. J., Xiao, M., and Xu, L., *Data Assimilation for Atmospheric, Oceanic and Hydrologic Applications*, Vol. 2, chap. 1: A Survey of Observers for Nonlinear Dynamical Systems, Springer, February 2013, pp. 1–25.